A Unique Diel Pattern in Carbonate Chemistry in the Seagrass Meadows of Dongsha Island: implications for ocean acidification buffering

Wen-Chen Chou[1,2*], Lan-Feng Fan[1], Chang-Chang Yang[1], Ying-Hsuan Chen[1], Chin-Chang Hung[3], Wei-Jen Huang[3], Yung-Yen Shih[3,4], Keryea Soong[3], Hsiao-Chun Tseng[1], Gwo-Ching Gong[1,2], Hung-Yu Chen[5], Cheng-Kuan Su[6]

[1]Institute of Marine Environment and Ecology, National Taiwan Ocean University, Keelung, Taiwan

[2]Center of Excellence for the Oceans, National Taiwan Ocean University, Keelung, Taiwan

[3]Department of Oceanography, National Sun Yat-sen University, Kaohsiung, Taiwan

[4]Department of Applied Science, R.O.C. Naval Academy, Kaohsiung, Taiwan

[5]Department of Marine Environmental Informatics, National Taiwan Ocean University, Keelung, Taiwan

[6]Department of Chemistry, National Chung Hsing University, Taichung, Taiwan

Corresponding author: Wen-Chen Chou (wcchou@mail.ntou.edu.tw)

Key Points:

- High pH values across a diel cycle seasonally occurred in the seagrass meadows of the semienclosed lagoon on Dongsha Island.
- The seagrass meadows of the semienclosed lagoon on Dongsha Island may create a localized buffering effect against ocean acidification.
- This effect may result from strong sedimentary alkalinity production induced by metabolic processes coupled with carbonate dissolution.

Abstract

In contrast to most seagrass meadows where seawater carbonate chemistry generally shows strong diel variations with a higher pH during the daytime and a lower pH during nighttime due to the alternation in photosynthesis and respiration, the seagrass meadows of the inner lagoon on Dongsha Island had a unique diel pattern with an extremely high pH across a diel cycle. We suggest that this distinct diel pattern in pH was a result of a combination of total alkalinity (TA) production through the coupling of aerobic/anaerobic respiration and carbonate dissolution in the sediments and dissolved inorganic carbon consumption through the high productivity of seagrasses in overlying seawaters. The confinement of the semienclosed inner lagoon may hamper water exchange and seagrass detritus export to the adjacent open ocean, which may provide an ideal scenario for sedimentary TA production and accumulation, thereby forming a strong capacity for seagrass meadows to buffer ocean acidification.

Plain Language Summary

As one of the most productive ecosystems on Earth, seagrass meadows may consume a large amount of carbon dioxide through photosynthesis and thus may have the potential to mitigate ocean acidification (OA) induced by rising atmospheric CO_2. However, previous studies have shown large diel and seasonal variability in seawater pH in seagrass meadows, suggesting that in a certain period of time, seagrass meadows cannot alleviate OA and may even exacerbate OA. In this study, we found a unique diel pattern with extremely high pH levels across a diel cycle in four different seasons, i.e., a yearly existing OA buffering capacity, within the seagrass meadows of the inner lagoon on Dongsha Island. Our data suggest that this extraordinary buffering capacity may result from strong sedimentary alkalinity production induced by the vigorous mechanistic coupling between metabolic processes and carbonate dissolution in this seagrass meadow in the semienclosed environment of the inner lagoon on Dongsha Atoll. To the best of our knowledge, the present study provides the first observational evidence showing that seagrass meadows in reef sediments may stimulate carbonate dissolution and thus alkalinity production, thereby constantly creating a localized buffering effect against OA.

1 Introduction

As one of the most productive ecosystems on Earth, seagrass meadows have been recognized for their important role in "blue carbon" storage (Duarte et al. 2010; Fourqurean et al., 2012). In addition to the significant carbon sequestration potential of seagrass meadows, recent studies have shown that the high level of seagrass primary productivity may alter seawater carbonate chemistry by consuming a large amount of dissolved inorganic carbon (DIC), thus, they may have the potential to mitigate ocean acidification (OA) induced by rising atmospheric CO_2 (Manzello et al., 2012; Unsworth et al., 2012; Pacella et al., 2018).

Carbonate chemistry dynamics in the water column of seagrass meadows is driven by a variety of metabolic activities, including plant photosynthesis/respiration (Semesi et al., 2009), carbonate formation/dissolution (Burdige et al, 2008, Howard et al, 2018; Saderne et al, 2019), benthic metabolism (Berg et al., 2019), and hydrodynamic processes (Ruesink et al., 2015). As a result, the carbonate system in the overlying water column of seagrass meadows generally shows large variabilities at diel and tidal time scales as well as seasonal variations (Waldbusser & Salisbury, 2014; Cyronak et al., 2018). In fact, several in situ investigations have revealed conflicting evidence as to whether seagrass meadows can buffer against OA. For instance, Challener et al. (2016) found significant diel and seasonal variability in seawater pH and the saturation state of aragonite (Ω_a) in a Florida seagrass meadow; the high pH and Ω_a values, which would alleviate OA, were observed during the daytime/growing season due to DIC uptake, while the low pH and Ω_a values, which would exacerbate OA, occurred during the nighttime/decay season due to DIC release. Furthermore, Hendriks et al. (2014) also reported diel pH changes in Mediterranean seagrass meadows, where the pH during 47% of the observation time was lower than the source seawater pH, suggesting a certain period of time when the seagrass meadows could not mitigate OA but exacerbated OA. These surveys clearly demonstrate that the OA buffering potential of seagrass meadows may have considerable temporal variability.

In contrast to most seagrass meadows, Chou et al. (2018) documented that the seagrass meadows of the inner lagoon on Dongsha Island in the South China Sea exhibited an exceptional diel pattern with an extremely high pH and low partial pressure of CO_2 (pCO_2) across a diurnal cycle during a 6-day survey. In this study, we revisited the same sites to examine whether this distinct diel pattern with an extremely high pH and low pCO_2 would repeatedly occur in all seasons. Moreover, we also collected sediment cores and porewater samples to clarify the potential role of sedimentary total alkalinity (TA) production in regulating the carbonate dynamics in the overlying waters. We found that the confinement of the semienclosed inner lagoon may provide an ideal scenario for sedimentary TA production, including high organic matter (OM) content, low sediment permeability and a long porewater residence time, thus distinguishing the seagrass meadows in the inner lagoon on Dongsha Island from those in the open environment.

2 Materials and Methods

2.1 Study sites

The study sites were the same as those in our previous work and have been comprehensively described in Chou et al. (2018). Briefly, the Dongsha Atoll is a circular coral reef located in the northern South China Sea (NSCS), and Dongsha Island is situated on the western margin of the atoll. A semienclosed inner lagoon occupies the central part of Dongsha

Island (Fig. 1). Two hydrodynamically contrasting seagrass meadows were chosen so that their diel cycles in seawater carbonate chemistry could be monitored. One meadow is located on the northern shore (NS), where water can freely exchange with the adjacent open ocean; the other is situated in the inner lagoon (IL), where water exchange is largely hampered due to confinement by a sand barrier. Previous surveys have revealed that both sites are multispecies seagrass meadows with the same dominant species (*Thalassia hemprichii* and *Cymodocea rotundata*; Lin et al., 2005) and similar coverages of seagrasses (81% ~85%; Huang et al., 2015).

2.2 Seawater and porewater samplings and carbonate chemistry and calcium ion analyses

Seawater samplings were conducted in January 2016 (1/1-12; winter), November 2016 (11/11-13; autumn), April 2018 (4/12-18; spring), and June-July 2019 (6/28-7/3; summer). During these sampling periods, seawater samples for carbonate chemistry analysis were taken at approximately 6:00 a.m., 12:00 a.m., and 18:00 p.m. every day. The sampling procedure and sample preservation are detailed in Chou et al. (2018). Measurements of TA, DIC, and pH followed the standard operating procedures described in Dickson et al. (2007), and the procedures were consistent with those used in our previous studies (Chou et al., 2018). Briefly, DIC and TA were determined using the nondispersive infrared method on a DIC analyzer (AS-C3, Apollo SciTech) and Gran titration on an automatic TA titrator (AS-ALK2, Apollo SciTech), respectively, and both measurements had accuracies and precisions of 0.2% or better. The pH was spectrophotometrically measured with a precision of 0.005. The partial pressure of CO_2 (pCO_2) was calculated from the measured DIC and TA data using the Excel macro CO2SYS version 2.1 (Pelletier et al., 2011).

Sediment cores and porewater samples were collected in the summer of 2019 at the IL, NS, and another unvegetated site located on the southern shore (SS; Fig. 1), which served as a reference site. Porewater samples were collected using porewater wells and modified from Falter & Sansone (2000). A total volume of 25 ml porewater was extracted from each well at 2, 4, 6, 8, 12, 16, and 20 cm sediment depths using a Luer-Lok syringe. The sampling procedure and sample preservation of porewater followed the methods in Kindeberg (2020). In addition to carbon chemistry parameters (TA, DIC, and pH), the calcium ion concentration of the porewater was determined using an ICP-MS system (Agilent 7700x, Agilent Technologies) based on that in Su & Ho (2019).

3 Results

3.1 Diel variations in carbonate chemistry

The seasonal diel variations in pH, pCO_2, DIC, and TA at the NS and IL sites are shown in Fig. 2. At the NS site (open squares), pH, pCO_2 and DIC showed distinct diel cycles in all seasons, which followed the diel pattern of photosynthesis and respiration; pH increased, but pCO_2 and DIC decreased during the day; and pH decreased, but pCO_2 and DIC increased during the night due to the daytime photosynthetic CO_2 uptake and nighttime respiratory CO_2 release. In contrast, TA did not show a clear diel cycle in all seasons, except that a weak diel pattern occurred in winter, with an increase at night but a decrease during the day (Fig. 2m). At the IL site (solid circle), similar diel variability was found for pH, pCO_2 and DIC; however, the amplitudes of variation were generally much smaller than those at the NS site, and TA did not reveal an obvious diel cycle.

The horizontal bands superimposed on Fig. 2a–d, 2i–l, and 2m–p represent the seasonal variation ranges of pH, DIC, and TA, respectively, in the NSCS, which were collected from the SouthEast Asian Time-series Study (SEATS) station at 18°N and 116°E (Tseng et al., 2007). The horizontal dashed lines shown in Fig. 2e-h denote the atmospheric pCO_2 (400 μatm). As shown, at the NS site, the pH was generally higher than the published ranges in the NSCS from midday to midnight; however, the pH was lower from midnight to midday in all seasons, and the opposite pattern was found for DIC. Similarly, pCO_2 was lower than the atmospheric pCO_2 from midday to midnight, while it was higher from midnight to midday in all seasons, except in spring, when pCO_2 across a diel cycle was almost always lower than the atmospheric pCO_2. TA across a diel cycle was generally higher than the published range, except in summer, when TA varied within the published range. In contrast, at the IL site, the pH across a diel cycle was higher than the published range, while the pCO_2 across a diel cycle was lower than the atmospheric pCO_2 in all seasons, suggesting yearly existing OA buffering and atmospheric CO_2 absorbing capacities for the seagrass meadows in the IL on Dongsha Island. Furthermore, DIC across a diel cycle was generally lower than the published range, except in fall when DIC was higher. In contrast, TA across a diel cycle was almost always higher than the published TA range in all seasons.

3.2 Porewater carbonate chemistry and calcium ion concentration

The vertical porewater profiles of the carbonate parameters and calcium ion concentrations at the SS, NS and IL sites are shown in Fig. 3a–f. Overall, porewater DIC, TA and pCO_2 profiles showed an increasing trend with sediment depth, and values were generally greater in the porewater than in the overlying water column at all sites. In contrast, pH and Ω_a revealed a decreasing trend, and values were lower in the porewater than in the overlying water column. Nevertheless, the vertical gradients of the carbonate parameters differed strikingly among the different sites. The sharpest vertical gradients of porewater carbonate parameters were found at the IL site, where the average depth-integrated changes in DIC, TA, pCO_2, pH and Ω_a relative to the sediment-water interface (SWI) were +3408±1218 μM, +1788±865 μM, +25924±15775 μatm, –2.21±0.18 pH units and –11.64±0.73, respectively, and the smallest vertical gradients of carbonate parameters were observed at the unvegetated SS site, where the average depth-integrated changes in DIC, TA, pCO_2, pH and Ω_a were +71±23 μM, +21±28 μM, +149±75 μatm, –0.17±0.15 pH units and –0.52±0.31, respectively. The vertical profiles of the carbonate

parameters at the NS site were closer in magnitude to those at the unvegetated SS site than those at the IL site, where the average depth-integrated changes in DIC, TA, pCO_2, pH and Ω_a were +384±114 μM, +89±67 μM, +1529±627 μatm, –0.42±0.09 pH units and –2.87±0.57, respectively. Furthermore, it is worth noting that porewater below 2 cm at the IL site was generally undersaturated with respect to aragonite ($\Omega_a<1$; except at 12 cm), while porewater remained supersaturated ($\Omega_a>1$) throughout the entire profiles at the NS and SS sites (Fig. 3e).

The vertical profiles of calcium ion concentration in porewaters also differed markedly among the different sites. The calcium ion concentration remained fairly constant at 380–400 ppm throughout the entire profile at the SS and NS sites, while it gradually increased from the SWI to a maximum of 515 ppm at 12 cm and then decreased to 20 cm. Similar to those of the carbonate parameters, the average depth-integrated change in calcium ion concentration at the IL site (+34±33 ppm) was noticeably higher than those at the NS (+9±3 ppm) and SS (+8±6 ppm) sites.

4 Discussion

As revealed in the results, the CO_2 dynamics at the NS site showed strong diel variation in all seasons, which was similar to the common pattern found in most seagrass meadows (Bouillon et al., 2007; Turk et al., 2015; Ganguly et al., 2017; Cyronak et al., 2018; Berg et al., 2019; McCutcheon et al., 2019). In contrast, to the best of our knowledge, the seasonal recurrence of high pH and low pCO_2 values across a diel cycle at the IL site has never been documented in any marine ecosystem. We propose that the semienclosed setting of the IL may provide an ideal circumstance for sedimentary TA production that may be transferred to the overlying water column and drive elevated pH and depressed pCO_2, thereby forming the observed unique diel pattern in carbonate chemistry at the IL site.

Previous studies have shown that seagrasses may induce carbonate sediment dissolution by the combined effect of OM being supplied and oxygen pumping via their roots and rhizomes, which may fuel OM respiration and thus CO_2 release and a lower carbonate saturation state (Ω), consequently leading to carbonate mineral dissolution (Burdige & Zimmerman, 2002; Burdige et al., 2008; Kindeberg et al., 2020). This process is often referred to as "metabolic carbonate dissolution", as represented in the following equations:

$$CH_2O + O_2 \rightarrow CO_2 + H_2O \rightarrow H_2CO_3 \quad (1)$$

$$CaCO_3 + H_2CO_3 \rightarrow Ca^{2+} + 2HCO_3^- \quad (2)$$

where CH_2O represents a simplified formula for OM undergoing remineralization. The net reaction can therefore be described stoichiometrically as:

$$CH_2O + O_2 + CaCO_3 \rightarrow Ca^{2+} + 2HCO_3^- \quad (3)$$

which increases both the TA and DIC of the porewater with a ratio of 1:1.

Whereas aerobic respiration coupled with carbonate dissolution could be the dominant process controlling TA and DIC variations in porewater under oxygenated conditions, numerous redox reactions, including nitrate, manganese, iron and sulfate reductions, may occur throughout the sediment column under anoxic conditions, which may also significantly contribute to TA and DIC variations in porewater. As the concentrations of nitrate, manganese and iron are generally much lower than sulfate in seawater (especially for a pelagic ocean regime such as that at Dongsha Atoll due to the lack of terrestrial input), sulfate reduction typically represents a major OM remineralization pathway under anoxic conditions (Burdige, 2011), as denoted in the

following equation:

$$2CH_2O + SO_4^{2-} \rightarrow 2HCO_3^- + H_2S \qquad (4)$$

However, in shallow carbonate sediments, the resulting H_2S can largely reoxidize to sulfate within the oxic layer, which can produce acid and thus can also induce carbonate dissolution (Ku et al., 1999; Burdige et al., 2008; Drupp et al., 2016), as represented in the following equations:

$$H_2S + 2O_2 \rightarrow SO_4^{2-} + 2H^+ \qquad (5)$$

$$CaCO_3 + H^+ \rightarrow Ca^{2+} + HCO_3^- \qquad (6)$$

The net reactions in equations (4), (5) and (6) are identical to those occur from "metabolic carbonate dissolution", as denoted by equation (3). As a result, the coupling of sulfate reduction, sulfide oxidation, and carbonate dissolution may also simultaneously produce TA and DIC at a ratio of 1:1 (Burdige & Zimmerman, 2002).

Plots of TA against DIC are often used to interpret the processes controlling the carbonate system in porewater because the relative variation in TA and DIC follows a well-established stoichiometric ratio that is specific to the respective processes, where the ratios for aerobic respiration (AR, equation 1), sulfate reduction (SR, equation 4) and carbonate dissolution (CD, equation 2 and 6) are 0/1, 1/1 and 2/1, respectively (Hu & Cai, 2011; Rassmann et al., 2020). Furthermore, as explained earlier, a coupling between AR and CD and that between SR and CD result in TA and DIC variations of 1:1.

Fig. S1 shows the covariation in TA and DIC for the porewater collected below a 2 cm sediment depth (filled symbols) and the overlying water collected at the SWI (open symbols) at the IL, NS, and SS sites. As shown, the overlying water points are apparently offset from the regression lines at the IL and NS sites (black arrows in Fig. S1a & b), while this scenario is not evident at the SS site. This offset is very close to the specific stoichiometric relationship of AR, suggesting that AR of OM may dominate the initial DIC increase before CD can take place, leading to a TA increase. The slopes of TA *vs.* DIC of the regression lines for the IL and NS porewater are 0.70 and 0.51, respectively, while the porewater TA and DIC at the SS site did not exhibit significant linearity ($p=0.3849$). Neither slope follows the specific ratio of any single process, implying that AR and SR, both coupled with CD under oxic and anoxic conditions, may collectively control TA and DIC variations in porewater at the IL and NS sites (Drupp et al., 2016). Furthermore, the larger slope suggests that SR coupled with CD may exert a stronger influence on the variations in TA and DIC in porewater at the IL site than at the NS site. Additionally, DIC, TA and Ca^{2+} concentrations in porewater at the IL site were much higher than those at the NS site (Fig. 3), and the latter was slightly higher than those at the unvegetated SS site. These results provide further evidence to support the assertion that TA and DIC production, driven by the coupling among AR, SR and CD, may indeed occur in vegetated reef sediments, and these metabolic processes should have been much stronger at the IL site than at the NS site, although both sites were covered by the same dominant seagrass species (*Thalassia hemprichii* and *Cymodocea rotundata*; Lin et al., 2005) with similar coverage amounts and shoot densities (Huang et al., 2015).

We propose that the observed intensive sedimentary DIC and TA production at the IL site is likely due to a combination of higher OM content, lower sediment permeability and longer residence time of porewater there than at the other sites. The confinement of the semienclosed inner lagoon may hamper seagrass detritus export to the adjacent open ocean and thus cause more OM to accumulate in the reef sediments at the IL site (Fig. S2a and b). The elevated OM content may fuel DIC (H_2CO_3) production through AR (reaction 1 in Fig. 4), which may further

drive CD and thus generate TA and DIC (reaction 2 and 3 in Fig. 4). Moreover, the relatively calm hydrodynamic environment could also be favorable for fine-grained sediment accumulation at the IL site (Fig. S2c and d), which may facilitate TA and DIC production in several ways. First, fine-grained sediments can provide greater available reactive surface area for all of the metabolic processes. Second, the overall finer-grained sediments may result in a lower permeability, which may reduce oxygen penetration and thus favor the occurrence of anaerobic respiration (e.g., SR, reaction 4 in Fig. 4). The resulting sulfide may subsequently reoxidize within the shallow oxic layer (reaction 5 in Fig. 4), which may also induce CD (reaction 6 in Fig. 4). Finally, the less-energetic hydrodynamic and low sediment permeability may collectively result in a longer porewater residence time and thus allow for the buildup of DIC and TA in the porewater at the IL site.

The accumulated high TA and DIC in the porewater can then be transferred to the overlying water column via the advection induced by tide, current, and wave actions and/or the diffusion driven by the chemical gradient between the SWI. The transferred DIC can be taken up again through the high productivity of the seagrasses (i.e., photosynthesis; reaction 7 in Fig. 4), whereas photosynthesis cannot consume TA. Consequently, the TA transferred from porewater can remain in the overlying water column. The confinement of the IL site may also hinder water exchange with the adjacent open ocean, thus providing another favorable circumstance for the accumulation of the sedimentary generated TA in the overlying water column. Thermodynamically, TA increases with a constant DIC may not only drive pH increases and pCO_2 decreases in seawater but also enhance their buffer capacities. Accordingly, a weak diel pattern with an extremely high pH and low pCO_2 across a diurnal cycle was seasonally observed within the seagrass meadows at the IL site.

5 Concluding remarks

To the best of our knowledge, the seasonal recurrence of high pH and low pCO_2 values across a diel cycle within seagrass meadows, such as those at the IL site on Dongsha Island, has never been reported in any marine ecosystem. We suggest that this unique diel pattern in carbonate chemistry was a result of a combination of higher OM content, lower sediment permeability and longer residence time of the porewater at this site than at the other sites due to the confinement of the environmental setting, which may collectively provide an ideal circumstance for sedimentary TA production and its subsequent accumulation in the overlying water. Overall, our results demonstrate that strong mechanistic linkages exist between seagrass metabolic processes and TA production in reef sediments, and this mechanism can be enhanced in a semienclosed environmental setting, by which atmospheric CO_2 can be transferred to the oceanic carbonate and bicarbonate pool and thus can buffer OA and atmospheric CO_2 increases. Most importantly, the present study provides the first observational evidence showing that the intense mechanistic coupling between metabolic processes and carbonate dissolution in seagrass meadows may create a localized buffering effect against OA, and the magnitude of this effect merits more attention to better understand the role of coastal vegetated reef ecosystems in buffering OA.

Data Availability Statement

The data used for this study are available at PANGAEA (https://issues.pangaea.de/browse/PDI-26083), and can be found in the supporting information file.

Acknowledgments

We are grateful to the Dongsha Atoll Research Station, Dongsha Atoll National Park, and Coast Guard Administration for assistance in field sampling. We thank Rong-Wei Syu, Hui-Chuan Chu, and Kuan-Chieh Wu for their help with the laboratory work.

References

Berg, P., Delgard, M. L., Polsenaere, P., McGlathery, K. J., Doney, S. C., & Berger, A. C. (2019). Dynamics of benthic metabolism, O_2, and pCO_2 in a temperate seagrass meadow. *Limnology and Oceanography*, *64*(6), 2586-2604.

Bouillon, S., Dehairs, F., Velimirov, B., Abril, G., & Borges, A. V. (2007). Dynamics of organic and inorganic carbon across contiguous mangrove and seagrass systems (Gazi Bay, Kenya). *Journal of Geophysical Research-Biogeosciences, 112*(G2). http://dx.doi.org/10.1029/2006jg000325.

Burdige, D.J. (2011). BIOGEOCHEMISTRY, in Laane, R. and Middelburg, J.J. eds., Estuarine and coastal sediments–coupled biogeochemical cycling treatise on estuarine and coastal science. Elsevier Inc. Academic Press, 279-316.

Burdige, D. J., & Zimmerman, R. C. (2002). Impact of sea grass density on carbonate dissolution in Bahamian sediments. *Limnology and Oceanography*, *47*(6), 1751-1763. http://dx.doi.org/10.4319/lo.2002.47.6.1751.

Burdige, D. J., Zimmerman, R. C., & Hu, X. P. (2008). Rates of carbonate dissolution in permeable sediments estimated from pore-water profiles: The role of sea grasses. *Limnology and Oceanography*, *53*(2), 549-565. http://dx.doi.org/10.4319/lo.2008.53.2.0549.

Challener, R. C., Robbins, L. L., & McClintock, J. B. (2016). Variability of the carbonate chemistry in a shallow, seagrass-dominated ecosystem: Implications for ocean acidification experiments. *Marine and Freshwater Research*, *67*(2), 163-172. http://dx.doi.org/10.1071/mf14219.

Chou, W. C., Chu, H. C., Chen, Y. H., Syu, R. W., Hung, C. C., & Soong, K. (2018). Short-term variability of carbon chemistry in two contrasting seagrass meadows at Dongsha island: Implications for pH buffering and CO_2 sequestration. *Estuarine Coastal and Shelf Science, 210*, 36-44. http://dx.doi.org/10.1016/j.ecss.2018.06.006.

Cyronak, T., Andersson, A. J., D'Angelo, S., Bresnahan, P., Davidson, C., Griffin, A., et al. (2018). Short-term spatial and temporal carbonate chemistry variability in two contrasting seagrass meadows: Implications for ph buffering capacities. *Estuaries and Coasts, 41*(5), 1282-1296. http://dx.doi.org/10.1007/s12237-017-0356-5.

Dickson, A. G., Sabine, C. L., & Christian, J. R., 2007, Guide to best practices for ocean CO_2 measurements: North Pacific Marine Science Organization.

Drupp, P. S., De Carlo, E. H., & Mackenzie, F. T. (2016). Porewater CO_2-carbonic acid system chemistry in permeable carbonate reef sands. *Marine Chemistry, 185*, 48-64. http://dx.doi.org/10.1016/j.marchem.2016.04.004.

Duarte, C. M., Marba, N., Gacia, E., Fourqurean, J. W., Beggins, J., Barron, C., et al. (2010). Seagrass community metabolism: Assessing the carbon sink capacity of seagrass meadows. *Global Biogeochemical Cycles, 24*. http://dx.doi.org/10.1029/2010gb003793.

Falter, J., & Sansone, F. (2000). Shallow pore water sampling in reef sediments. *Coral Reefs, 19*(1), 93-97.

Fourqurean, J. W., Duarte, C. M., Kennedy, H., Marbà, N., Holmer, M., Mateo, M. A., et al. (2012). Seagrass ecosystems as a globally significant carbon stock. *Nature geoscience, 5*(7), 505-509.

Ganguly, D., Singh, G., Ramachandran, P., Selvam, A. P., Banerjee, K., & Ramachandran, R. (2017). Seagrass metabolism and carbon dynamics in a tropical coastal embayment. *Ambio, 46*(6), 667-679. http://dx.doi.org/10.1007/s13280-017-0916-8.

Hendriks, I. E., Olsen, Y. S., Ramajo, L., Basso, L., Steckbauer, A., Moore, T. S., et al. (2014). Photosynthetic activity buffers ocean acidification in seagrass meadows. *Biogeosciences, 11*(2), 333-346. http://dx.doi.org/10.5194/bg-11-333-2014.

Howard, J. L., Creed, J. C., Aguiar, M. V. P., & Fouqurean, J. W. (2018). CO_2 released by carbonate sediment production in some coastal areas may offset the benefits of seagrass "blue carbon" storage. *Limnology and Oceanography, 63*(1), 160-172. http://dx.doi.org/10.1002/lno.10621.

Hu, X., & Cai, W. J. (2011). An assessment of ocean margin anaerobic processes on oceanic alkalinity budget. *Global Biogeochemical Cycles, 25*(3).

Huang, Y. H., Lee, C. L., Chung, C. Y., Hsiao, S. C., & Lin, H. J. (2015). Carbon budgets of multispecies seagrass beds at Dongsha island in the South China sea. *Marine Environmental Research, 106*, 92-102. http://dx.doi.org/10.1016/j.marenvres.2015.03.004.

Kindeberg, T., Bates, N. R., Courtney, T. A., Cyronak, T., Griffin, A., Mackenzie, F. T., et al. (2020). Porewater carbonate chemistry dynamics in a temperate and a subtropical seagrass system. *Aquatic Geochemistry*). http://dx.doi.org/10.1007/s10498-020-09378-8.

Ku, T. C. W., Walter, L. M., Coleman, M. L., Blake, R. E., & Martini, A. M. (1999). Coupling between sulfur recycling and syndepositional carbonate dissolution: Evidence from oxygen and sulfur isotope composition of pore water sulfate, South Florida Platform, USA. *Geochimica Et Cosmochimica Acta, 63*(17), 2529-2546. http://dx.doi.org/10.1016/s0016-7037(99)00115-5.

Lin, H. J., Hsieh, L. Y., & Liu, P. J. (2005). Seagrasses of Tongsha island, with descriptions of four new records to Taiwan. *Botanical Bulletin of Academia Sinica, 46*(2), 163-168.

Manzello, D. P., Enochs, I. C., Melo, N., Gledhill, D. K., & Johns, E. M. (2012). Ocean acidification refugia of the Florida reef tract. *Plos One, 7*(7). http://dx.doi.org/10.1371/journal.pone.0041715.

McCutcheon, M. R., Staryk, C. J., & Hu, X. P. (2019). Characteristics of the carbonate system in a semiarid estuary that experiences summertime hypoxia. *Estuaries and Coasts, 42*(6), 1509-1523. http://dx.doi.org/10.1007/s12237-019-00588-0.

Pacella, S. R., Brown, C. A., Waldbusser, G. G., Labiosa, R. G., & Hales, B. (2018). Seagrass habitat metabolism increases short-term extremes and long-term offset of CO_2 under future ocean acidification. *Proceedings of the National Academy of Sciences of the United States of America, 115*(15), 3870-3875. http://dx.doi.org/10.1073/pnas.1703445115.

Pelletier, G., Lewis, E., & Wallace, D. (2011). CO2SYS. XLS: A calculator for the CO_2 system in seawater for microsoft Excel/VBA. Version 16. *Washington State Department of Ecology*).

Rassmann, J., Eitel, E. M., Lansard, B., Cathalot, C., Brandily, C., Taillefert, M., et al. (2020). Benthic alkalinity and dissolved inorganic carbon fluxes in the Rhone River prodelta generated by decoupled aerobic and anaerobic processes. *Biogeosciences, 17*(1), 13-33. http://dx.doi.org/10.5194/bg-17-13-2020.

Ruesink, J. L., Yang, S., & Trimble, A. C. (2015). Variability in carbon availability and eelgrass (Zostera marina) biometrics along an estuarine gradient in Willapa Bay, WA, USA. *Estuaries and Coasts, 38*(6), 1908-1917. http://dx.doi.org/10.1007/s12237-014-9933-z.

Saderne, V., Geraldi, N. R., Macreadie, P. I., Maher, D. T., Middelburg, J. J., Serrano, O., et al. (2019). Role of carbonate burial in blue carbon budgets. *Nature Communications, 10*. http://dx.doi.org/10.1038/s41467-019-08842-6.

Semesi, I. S., Beer, S., & Bjork, M. (2009). Seagrass photosynthesis controls rates of calcification and photosynthesis of calcareous macroalgae in a tropical seagrass meadow. *Marine Ecology Progress Series, 382*, 41-47. http://dx.doi.org/10.3354/meps07973.

Su, C.-K., & Ho, C.-C. (2019). Online profiling of living rat brain extracellular ph using a pH-dependent solid phase extraction scheme coupled with microdialysis sampling and inductively coupled plasma mass spectrometry. *Analytica Chimica Acta, 1055*, 36-43.

Tseng, C. M., Wong, G. T. F., Chou, W. C., Lee, B. S., Sheu, D. D., & Liu, K. K. (2007). Temporal variations in the carbonate system in the upper layer at the SEATS station. *Deep-Sea Research Part Ii-Topical Studies in Oceanography, 54*(14-15), 1448-1468. http://dx.doi.org/10.1016/j.dsr2.2007.05.003.

Turk, D., Yates, K. K., Vega-Rodriguez, M., Toro-Farmer, G., L'Esperance, C., Melo, N., et al. (2015). Community metabolism in shallow coral reef and seagrass ecosystems, lower Florida Keys. *Marine Ecology Progress Series, 538*, 35-52. http://dx.doi.org/10.3354/meps11385.

Unsworth, R. K. F., Collier, C. J., Henderson, G. M., & McKenzie, L. J. (2012). Tropical seagrass meadows modify seawater carbon chemistry: Implications for coral reefs impacted by ocean acidification. *Environmental Research Letters, 7*(2). http://dx.doi.org/10.1088/1748-9326/7/2/024026.

399 Waldbusser, G. G., & Salisbury, J. E. (2014). Ocean acidification in the coastal zone from an organism's
400 perspective: Multiple system parameters, frequency domains, and habitats. *Annual Review of Marine*
401 *Science*, 6, 221-247.

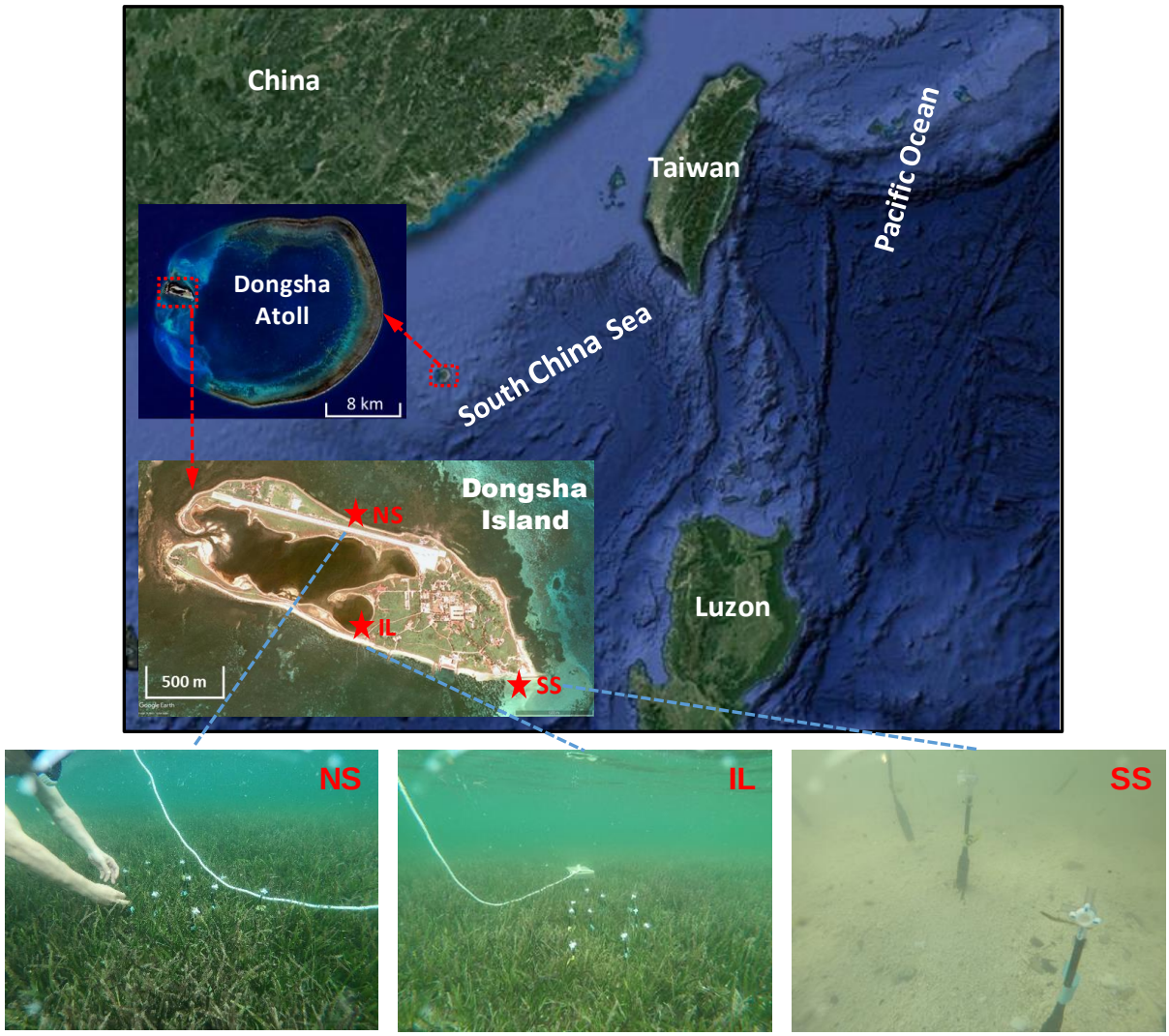

Fig. 1 Map showing the locations of Dongsha Atoll, Dongsha Island, and the sampling sites around Dongsha Island (upper panels) and photos showing the porewater sampling sites on the northern shore (NS), in the inner lagoon (IL), and on the southern shore (SS) (lower panels).

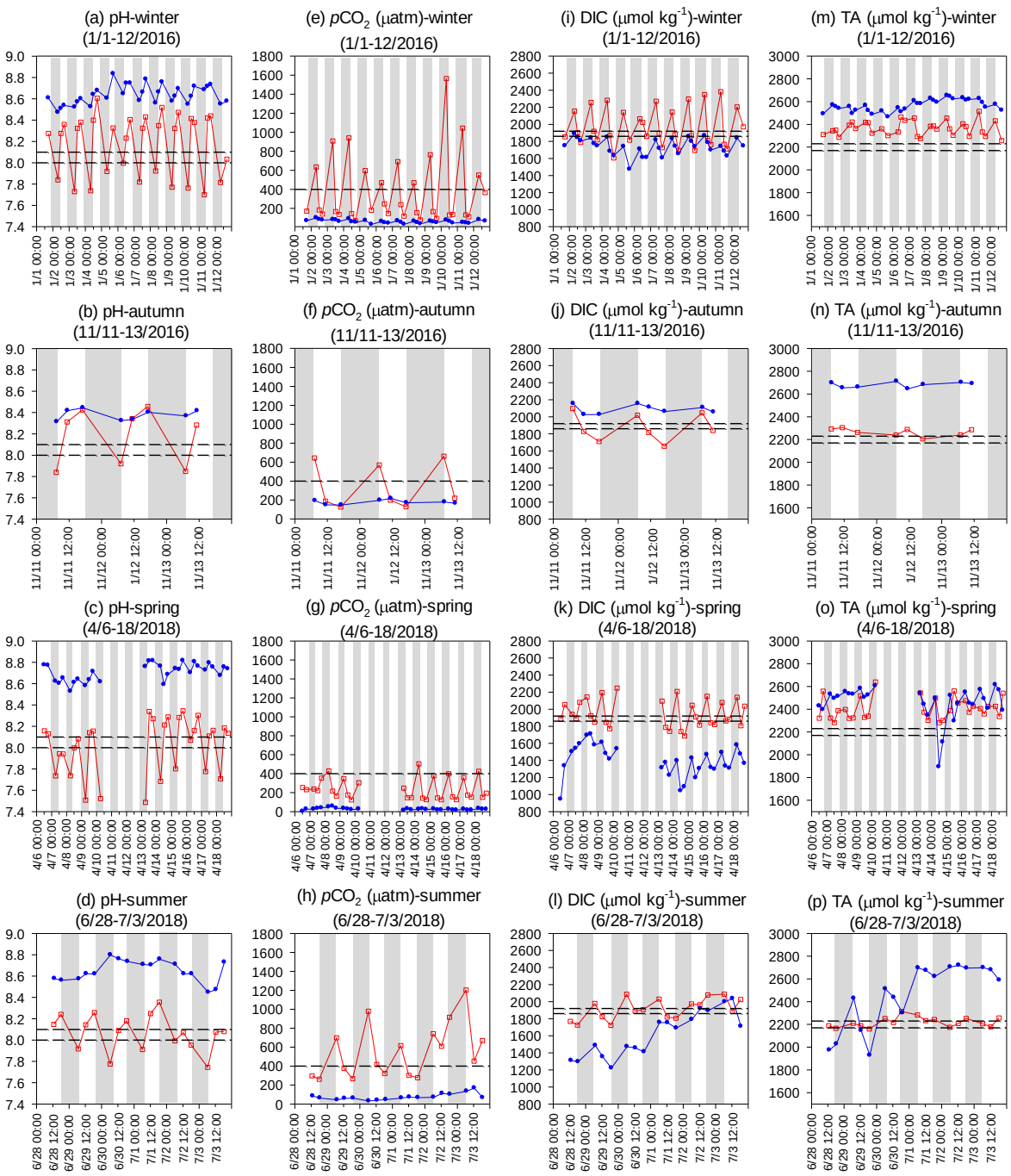

Fig. 2 Seasonal diel variations in (a–d) pH, (e–h) pCO_2, (i–l) DIC, and (m–p) TA in the inner lagoon (IL, solid circles) and on the northern shore (NS, open squares) of Dongsha Island. The white and gray areas represent daytime (06:00–18:00) and nighttime (18:00–06:00), respectively. The horizontal bands superimposed on Fig. 2a–d, 2i–l, and 2m–p represent the seasonal variation ranges in pH, DIC, and TA, respectively, in the open northern South China Sea. The horizontal dashed lines shown in Fig. 2e–h denote atmospheric pCO_2 (400 µatm).

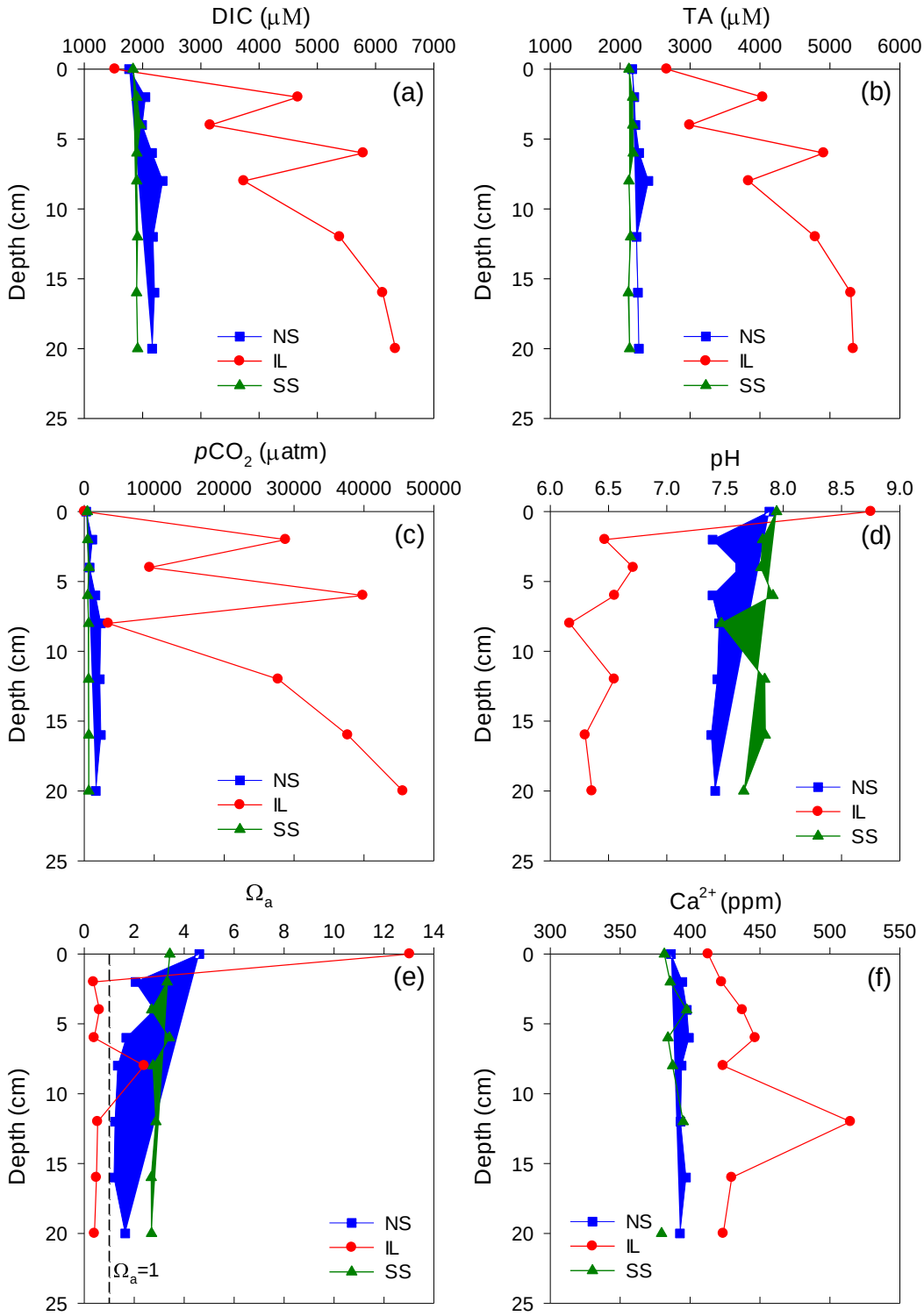

Fig. 3 Vertical porewater profiles of (a) DIC, (b) TA, (c) pCO_2, (d) pH, (e) Ω_a, and (f) Ca^{2+} on the northern shore (NS, square), in the inner lagoon (IL, circle), and on the southern shore (SS, triangle) of Dongsha Island.

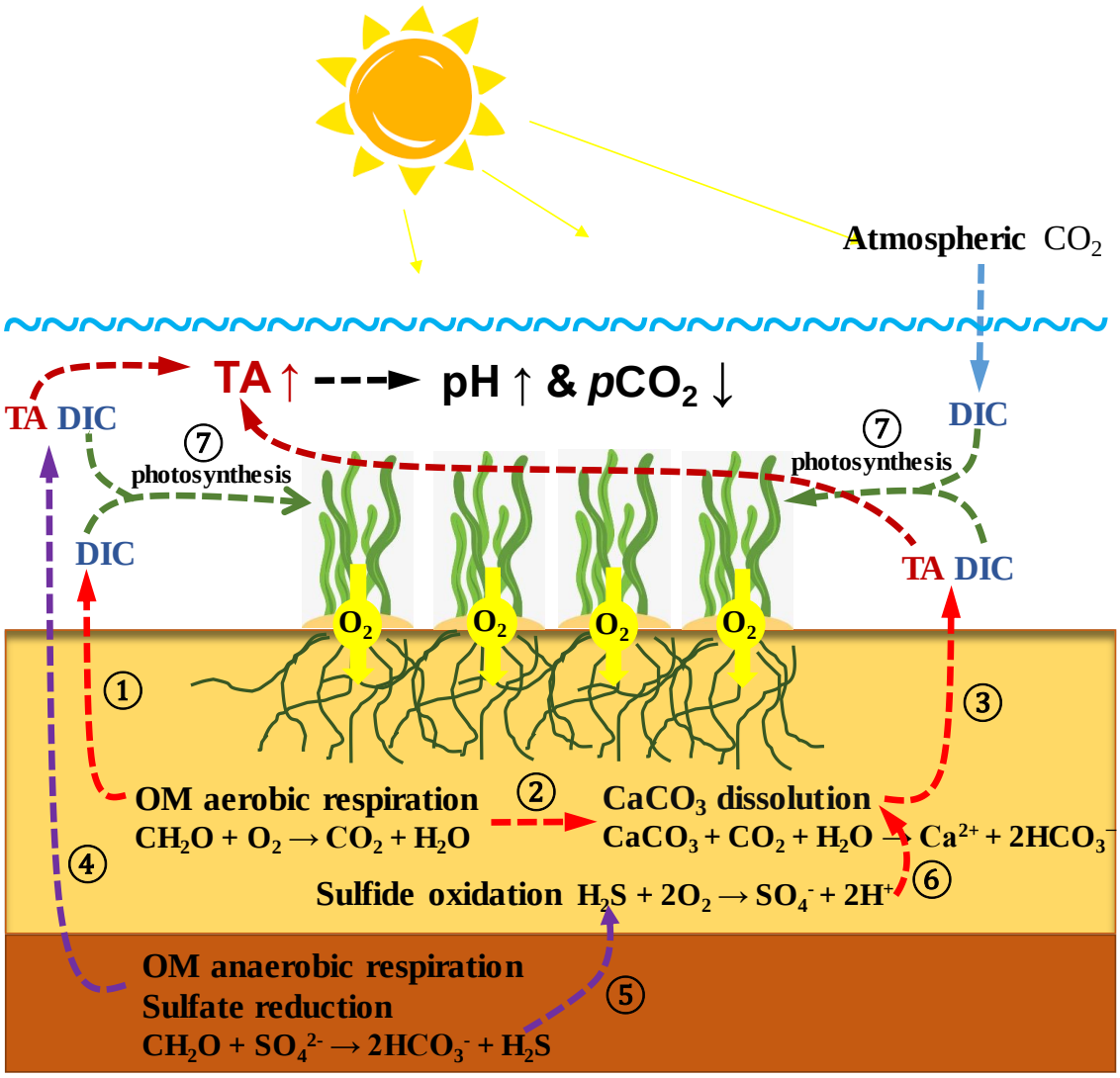

Fig. 4 Schematic representation of the key processes controlling porewater TA and DIC dynamics, which may collectively enhance sedimentary TA production and thereby forming a unique diel pattern with extremely high pH and low pCO_2 values across a diel cycle in the overlying seawater within the seagrass meadows of the inner lagoon on Dongsha Island.